The College of Engineering
University of Wisconsin-Madison

Wisconsin Electric Machines and Power Electronics Consortium

RESEARCH REPORT
88-12

POWER CAPABILITY OF SALIENT POLE PERMANENT MAGNET SYNCHRONOUS MOTORS IN VARIABLE SPEED DRIVE APPLICATIONS

Rich Schiferl and Thomas A. Lipo
Dept. of Electrical & Computer Engineering
University of Wisconsin-Madison
1415 Johnson Drive
Madison, WI 53706-1691

WEMPEC

Department of Electrical and Computer Engineering
1415 Johnson Drive
Madison, Wisconsin 53706

POWER CAPABILITY OF SALIENT POLE PERMANENT MAGNET SYNCHRONOUS MOTORS IN VARIABLE SPEED DRIVE APPLICATIONS[1]

Rich Schiferl, Member, IEEE
T. A. Lipo, Fellow, IEEE
University of Wisconsin
Electrical and Computer Engineering Department
1415 Johnson Drive
Madison, Wisconsin 53706-1691

Abstract- A constant parameter equivalent circuit model which neglects motor losses is used to determine the effects of dq reactances and open circuit voltage on the power capability of salient pole permanent magnet motors in variable speed drive applications. It is shown that peak power capability over a range of speeds can be obtained by proper control of the armature current magnitude and phase. Due to the voltage constraint imposed at the motor terminals the power capability will fall to zero for most motor designs at a given high speed. A simple relationship between the motor open circuit voltage and the direct axis reactance is derived to obtain motor designs that, even with this voltage constraint in place, extend their theoretical power capability, neglecting losses, to infinite speed. All results are presented in normalized curves using a per unit system.

I. INTRODUCTION

Salient pole permanent magnet synchronous motors can be constructed by either burying the magnets within the rotor iron or by placing them in slots on the rotor surface. In either case magnetic saliency is a result of low permeability magnets lying in the rotor direct axis flux paths while the quadrature axis paths lie entirely in iron.

A variety of rotor geometries of the buried magnet type are possible [1,2,6] where the space above the magnets may be used for a cage winding for line start purposes. In variable speed drive applications, however, the cage is not needed since motor starting can be achieved by ramping the inverter frequency. A typical example of a buried magnet rotor geometry is shown in Fig. 1(a). Steady state analysis techniques for determination of circuit parameters of buried magnet motors using classical rotating machine analysis methods and finite element field modelling are described in [1] and [9], respectively.

Control laws for variable speed drive operation of the buried magnet motor for both the constant torque (low speed) and constant power (flux weakening) operating modes are described in [3] and [4] for a given set of motor parameters. Little emphasis has been placed on the choice and influence of motor parameters on system performance in variable speed drive applications although in [5] it was suggested that the saturation dependent cross coupling effects in the buried magnet motor can enhance the power capability at high speed. These claims were contested in a later publication [10] in which it was shown that for some buried magnet motors the cross coupling effect disappears at low flux, high speed operating conditions.

Surface magnet, salient pole, permanent magnet synchronous motors can be realized by placing the magnets in slots on the rotor surface as shown in Fig. 1(b). This type of rotor construction is well suited for the new neodymium iron boron magnets since a high level of fundamental component air gap flux can be realized with the high field magnets and a magnet arc that is less than the pole pitch [7,8]. Steady state analysis methods for these inset magnet motors were described in [8] for variable speed drive operation with a current controlled inverter where it was reported that an increase in power capability at all speeds could be obtained with the salient pole design over that obtained from a protruding magnet design without iron between the magnet arcs. As with the buried magnet design, no detailed investigation of the effects of salient pole motor parameters on variable speed performance for the surface magnet designs has been reported.

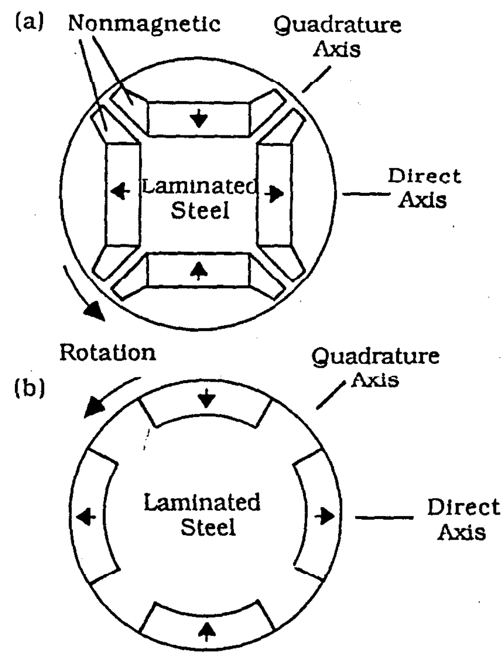

Fig. 1. Four pole rotors for salient pole permanent magnet motors. (a) Buried magnets, (b) Surface magnets.

The goal of this paper is to establish the relationship between steady state equivalent circuit parameters of salient pole permanent magnet motors and their power capability over a wide speed range. In all cases it will be assumed that the motor is supplied from a variable frequency inverter with current and rotor position feedback so that both current magnitude and phase (with respect to the rotor magnetic axes) can be independently controlled. Typical examples of such a drive system are given in [3], [4] and [8]. The system performance will be measured primarily by the shape of the motor power capability curve which is a plot of the maximum power attainable versus motor speed, subject to current and voltage magnitude constraints. A simple equivalent circuit model will be used in order to determine the best choice of motor circuit parameters necessary for power capability over a wide speed range. Throughout the analysis the optimal current angle for peak torque per amp operation will be discussed.

[1] This work was sponsored in part by the Wisconsin Electric Machines and Power Electronics Consortium (WEMPEC).

II. THE MOTOR MODEL

The steady state performance of salient pole permanent magnet machines is most accurately modelled by circuit equations with magnet flux linkage and armature reaction inductances that are nonlinear functions of the machine flux level. A large amount of insight into their steady state behavior in variable speed applications can be gained, however, by using a simplified model which neglects magnetic saturation and results in constant equivalent circuit inductances and magnet flux linkage. The analysis can be further simplified by neglecting all of the motor losses (copper, core and mechanical). (The effects of these assumptions will be discussed in part VII below). Assuming sinusoidally distributed stator windings and neglecting the air gap space harmonics induced by the magnet and armature reaction fields the resulting equivalent circuit model is most easily derived in the rotor d-q reference frame. These equations will be presented in their per unit form with base values of voltage and current chosen as the rated values for the motor at rated speed so that one per unit output power will correspond to motor operation at rated VA and unity power factor (i. e. the maximum possible output power attainable from this machine within the voltage and current rating).

Neglecting losses and saturation the steady state, per unit, dq axis voltage equations at any speed are

$$V_{qs} = n_{pu}(E_0 + X_{ds}I_{ds}) \text{ and} \tag{1}$$

$$V_{ds} = - n_{pu}X_{qs}I_{qs} \ , \tag{2}$$

where:
- n_{pu} = per unit speed,
- E_0 = per unit open circuit voltage at one per unit speed,
- X_{ds} = per unit direct axis reactance at one per unit speed,
- X_{qs} = per unit quadrature axis reactance at one per unit speed

and the direct and quadrature magnetic axes are as defined in Fig. 1.

With V_s defined as the a phase stator voltage phasor and I_s as the a phase line current phasor (defined as positive into the machine) the d and q axis components can be directly related to terminal quantities as

$$V_s = V_s\angle\delta = V_{qs} - jV_{ds} \tag{3}$$

$$I_s = I_s\angle\gamma = I_{qs} - jI_{ds} \, . \tag{4}$$

For a given current phasor (I_s) and open circuit voltage (E_0) the motor phasor diagram can be drawn as shown in Fig. 2.

The shaft output power equals the terminal input power in the lossless motor model and can be expressed in per unit as

$$P_{out} = V_{qs}I_{qs} + V_{ds}I_{ds} \tag{5}$$

or

$$P_{out} = n_{pu}\left[E_0 I_s \cos\gamma + \frac{X_{qs} - X_{ds}}{2} I_s^2 \sin 2\gamma \right] . \tag{6}$$

The output power has two components which can be identified as that resulting from magnet flux and armature current interaction ($E_0I_s\cos\gamma$) and that which is a result of the rotor saliency ($(X_{qs}-X_{ds})I_s^2\sin 2\gamma/2$). Output power is directly proportional to shaft speed for a given stator current and current angle.

For salient pole permanent magnet motors X_{ds} is less than X_{qs} since the direct axis armature reaction flux path contains the permanent magnets which usually have a relative permeability close to unity. The magnets, in effect, create a large air gap in the direct axis of the rotor. In contrast, the quadrature axis flux paths in the rotor are mostly in iron since the q axis armature reaction flux passes over the magnets in the buried magnet motor [3] and under the magnets in the surface magnet motor. The result of the magnetic saliency is that X_{ds} is less than X_{qs} and the saliency term in the power equation is positive for $0 < \gamma < 90°$. Consequently, maximum output power for a given I_s occurs for a current angle larger than zero. Peak power output at any speed can be obtained with rated current (one per unit) operation at this optimal current angle which will be called γ^*.

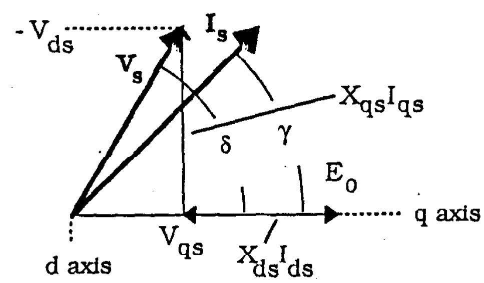

Fig. 2. Phasor diagram for a salient pole permanent magnet motor at one per unit speed.

III. POWER CAPABILITY AT LOW SPEEDS

Fig. 3 shows plots of the optimal current angle, γ^*, as a function of open circuit voltage and rotor saliency (X_{qs} - X_{ds}) for rated speed operation with one per unit line current. The corresponding maximum output power (or peak per unit torque) for operation at γ^* is plotted in Fig. 4. Rotor saliency near one per unit is not uncommon for either surface [11] or buried magnet [5] motors in integral horsepower designs.

Nonsalient pole rotor designs with $X_{qs} = X_{ds}$, which are most easily obtained in surface magnet machines, will provide maximum output power per amp with all of the armature current in the quadrature axis (i. e. $\gamma = 0°$). For these motors the peak output power is directly proportional to E_0. The magnet flux which creates E_0 is directly related to the size and the remanent flux density of the magnets. Generally speaking, magnet costs increase with increasing E_0 so there is an advantage to trading some magnet flux created power for rotor saliency created power. As shown in

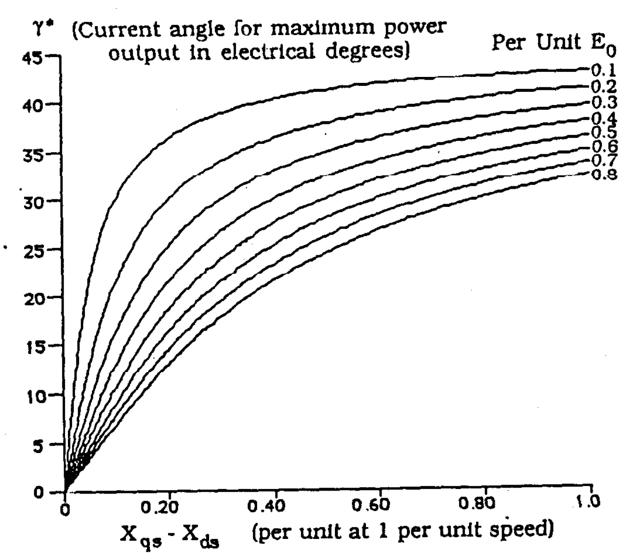

Fig. 3. Current angle for peak output power of salient pole permanent magnet machines at one per unit speed and current.

Fig. 4, a design with one per unit saliency and an E_0 of 0.4 per unit will have the same peak torque capability as a nonsalient pole design with nearly twice the value of E_0. The salient pole design would achieve peak torque at rated current for a current angle of about 37°. As can be seen from (6) this optimal current angle is a function of the motor current (or shaft load). Some cost advantage of the salient pole design (with less magnet) may be offset by the increase in complexity of the inverter in order to reach these optimal stator current angles at all speeds and power levels.

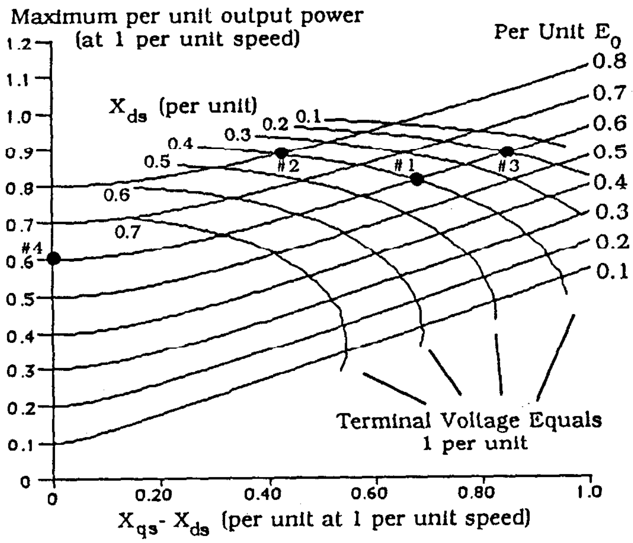

Fig. 4. Maximum output power at rated speed for salient pole permanent magnet machines with one per unit current.

IV. VOLTAGE LIMIT CONSTRAINTS ON POWER CAPABILITY

The peak power curves in Fig. 4 are derived assuming one per unit current and operation at the optimal current angle. In reality operation at this particular angle may not be realizable due to terminal voltage constraints. The per unit voltage can be obtained at any operating point from equations (1) and (2) as

$$V_{pu} = \sqrt{V_{qs}^2 + V_{ds}^2} = n_{pu}\sqrt{(E_0 - X_{ds}I_s\sin\gamma)^2 + (X_{qs}I_s\cos\gamma)^2} \quad (7)$$

The terminal voltage is directly proportional to the speed for a given stator current magnitude and angle so that the voltage constraint becomes more important at high motor speeds. At one per unit speed the one per unit voltage constraint is represented by curves of constant X_{ds} values in Fig. 4. Motor designs which lie on these curves will produce thier maximum output power at rated speed and current at the rated terminal voltage. Designs which fall to the left of their corresponding X_{ds} line will produce maximum output power (or optimal torque per amp) at one per unit speed for a terminal voltage less than one per unit. Designs which fall to the right of the line will not be able to produce maximum torque per amp under rated current and speed operation without exceeding the motor voltage rating. It appears that motor designs with low X_{ds} values will result in higher rated speed output power capability than those with higher per unit X_{ds} values.

A. Derivation of power capability curves

The terminal voltage is linearly related to speed so that at low speeds the rated voltage constraint does not prohibit motor operation at the peak output power (or maximum torque per amp) current angle (γ^*). As the speed increases the voltage constraint becomes more restrictive so that the rated current, peak output power operating point occurs for γ values which lie between γ^* and 90°. Fig. 5 shows terminal voltage and output power curves as a function of the current angle for ten different motor speeds for a motor design corresponding to point #1 in Fig. 4. All ten curves are for a one per unit stator current. At any given speed the terminal voltage decreases as γ increases since d axis armature reaction ($X_{ds}I_s\sin\gamma$ in (7)) opposing the magnet voltage (E_0) increases while q axis armature reaction ($X_{qs}I_s\cos\gamma$) decreases as γ goes from zero to 90 degrees. Below base speed the terminal voltage is less than one per unit at the optimal current angle so peak output power, which is linearly related to speed, is obtained for a constant current angle of γ^*. Above base speed the voltage constraint causes peak output power to be obtained at one per unit voltage and current for $\gamma > \gamma^*$ as peak power γ increases toward 90° where P_{out} is zero. Peak output power still increases with speed above one per unit speed (but no longer linearly with speed) until around two per unit speed where the maximum output power at any speed is obtained. At this speed one per unit output power is obtained at unity power factor.

The maximum output power attainable at a speed where operation at $\gamma = \gamma^*$ results in greater than one per unit terminal voltage can be obtained by finding the output power at the γ where the terminal voltage is one per unit as shown in Fig. 5. Repeating this procedure for all speeds results in the power capability curve shown in Fig. 6(a). This curve represents the theoretical limit on the output power of this motor at all speeds for rated current operation with the voltage limited to one per unit. Any power output below the curve can be obtained by reducing the stator current below its rated value and/or by advancing the current phase angle. Notice that for this particular motor design the output power

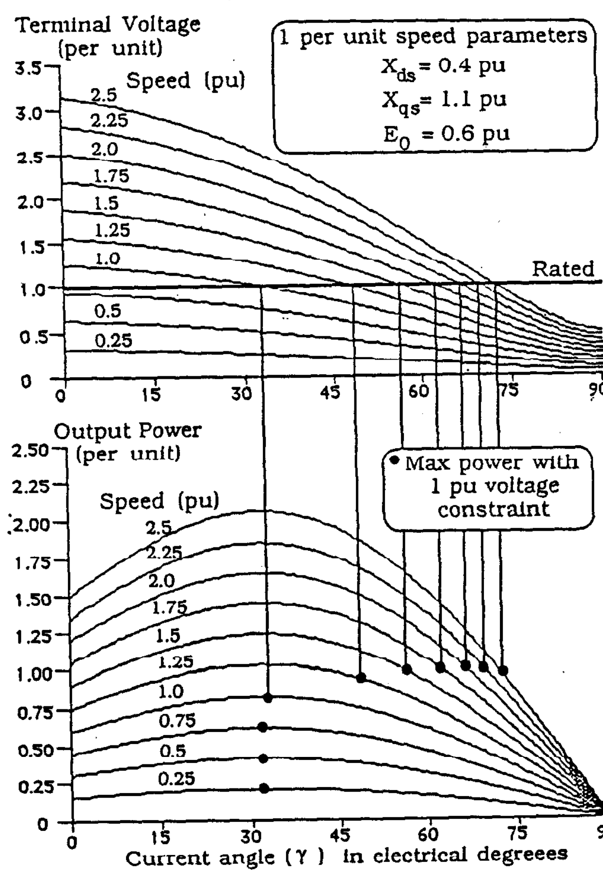

Fig. 5. Terminal voltage and power output for motor design #1 with 1 per unit current.

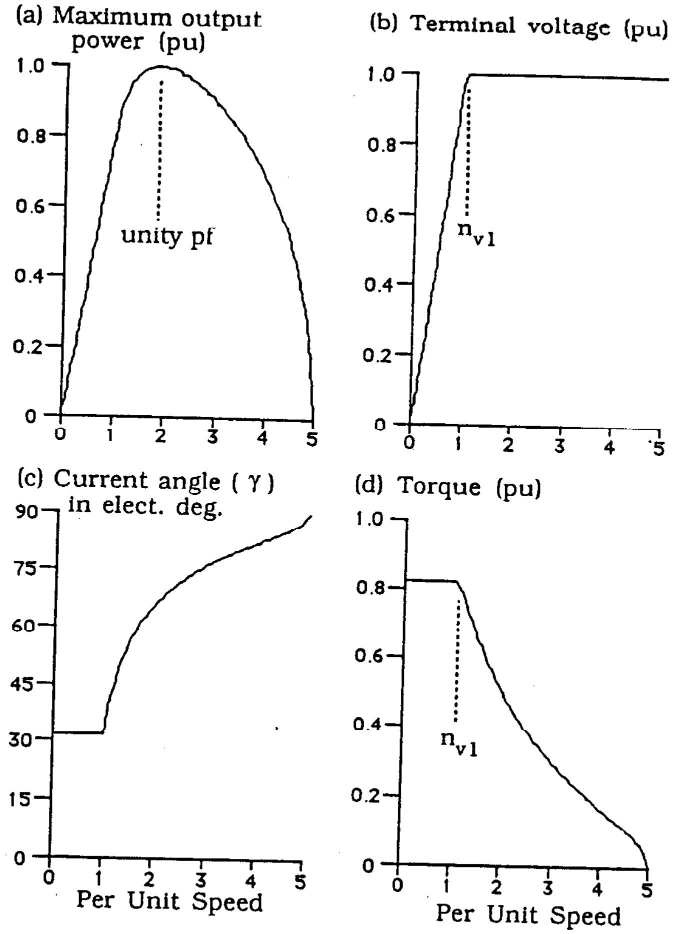

Fig. 6. Operating characteristics at maximum power output for motor design #1 with $X_{ds} = 0.4$, $X_{qs} = 1.1$ and $E_0 = 0.6$ per unit and 1 per unit current.

capability drops to zero at five times rated speed where the motor voltage is greater than one per unit for all values of γ.

Fig. 6 also contains graphs of current angle, terminal voltage and per unit torque for peak output power operation at all speeds. At low-speeds the terminal voltage increases linearly with speed (in a constant volts per hertz mode) as the current angle is held constant to achieve maximum torque per amp. Per unit torque remains at this maximum value until the terminal voltage reaches one per unit at a speed denoted as n_{v1} in Fig. 6(b) and (d). Above n_{v1} the torque begins to decrease (although the power increases until nearly two per unit speed) as the current is phase advanced to obtain flux weakening operation.

Fig. 7 shows phasor diagrams at four speeds for the motor design of Fig. 6. At low speeds the voltage and current phasor remain at constant angles for maximum torque per amp operation. Above base speed the current is phase advanced (I_s rotates counterclockwise) and the voltage phasor rotates clockwise (δ decreases) until at high speed all of the armature voltage rotates to the q axis where output power drops to zero. In general, for this particular motor design, the motor goes from lagging to leading power factor as the speed increases. Unity power factor operation results in one per unit output power and occurs around 2 per unit speed.

Power capability curves for any combination of motor parameters can be obtained by the method described above. Fig. 8 shows power capability curves for designs corresponding to points #1 through #4 in Fig. 4. Generally speaking; high open circuit voltage or low direct axis reactance (designs #2 and #3) result in limited power capability at high speed. These designs do provide

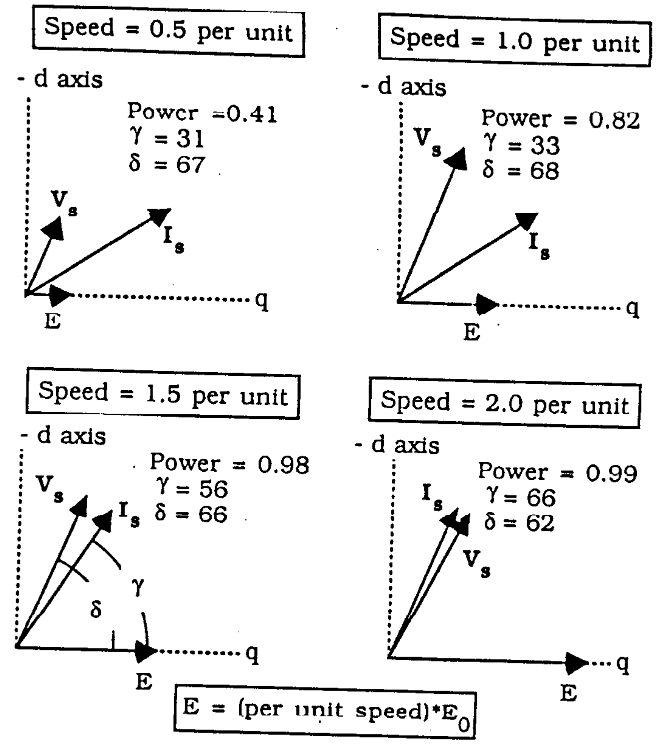

Fig. 7. Phasor diagrams for maximum power output operation of motor design #1 with $X_{ds} = 0.4$, $X_{qs} = 1.1$, and $E_0 = 0.6$ per unit.

(per unit at 1 per unit speed)

Design	X_{ds}	X_{qs}	E_0	$X_{qs} - X_{ds}$
# 1	0.4	1.10	0.6	0.70
# 2	0.4	0.84	0.8	0.44
# 3	0.2	1.05	0.6	0.85
# 4	0.4	0.40	0.6	0.0

Terminal voltage limited to 1 per unit at all speeds.

Maximum output power (pu) with 1 pu current

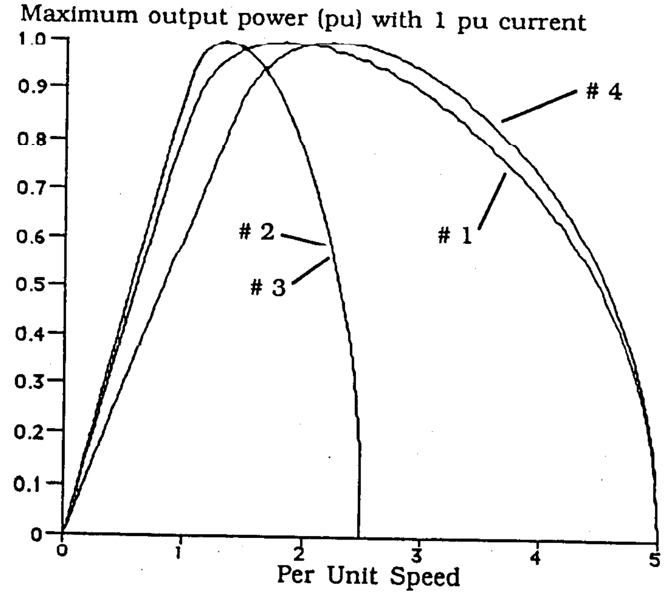

Fig. 8. Power capability curves for the four motor designs indicated in Fig. 4 with one per unit current.

the highest power capability (or maximum output torque) at low speeds so it appears that a tradeoff exists between power capability over a wide speed range and peak torque capability at low speeds.

B. Speed limit of peak torque output

Constant torque at maximum torque per amp is attainable up to the speed where volts per hertz control must be abandoned because of the voltage limit. This upper speed limit (n_{vl} in Fig. 6) represents the speed range over which peak output torque can be maintained. Fig. 9 shows the relationship between n_{vl} and the motor circuit parameters for motor designs with three different open circuit voltage values. As the direct axis reactance, open circuit voltage or rotor saliency increases the speed range for constant torque operation decreases. Comparison of Fig. 9 with Fig. 4 suggests that a tradeoff exists between motor peak torque capability and the speed range over which this peak torque can be maintained subject to the voltage constraint.

V. DESIGN RULE FOR POWER CAPABILITY OVER A WIDE SPEED RANGE

In the previous section it was shown that the choice of equivalent circuit parameters has an influence on the shape of the power capability curve over a wide speed range. All four motor designs in Fig. 8 had power capability curves which went to zero at some speed above rated speed. This maximum speed appears to be a strong function of the equivalent circuit parameters. Given complete freedom of choice of equivalent circuit parameters it is conceivable that an optimal set of X_{qs}, X_{ds} and E_0 values exists in order to obtain substantial power output at high speed. The question remains as to what criterion should be used to measure optimal motor performance. One obvious choice would be to choose a design which produces a given output power at rated speed and at some predetermined high speed value. Given these two power requirements the three circuit parameters could be optimized to obtain the desired objective. This approach will no doubt result in several "optimal" sets of parameters.

A more generalized approach can be used to evaluate motor power capability by considering a less specific optimization objective. Consider the power capabilty curves for the four specific motor designs in Fig. 8. All four designs have power capability dropping to zero at some speed above base speed. This occurs when the stator current angle (γ) reaches 90°. Above this speed the motor is incapable of providing output power without having the terminal voltage rise above one per unit (or its rated value). Power capability at high speed is directly related to the speed at which the theoretical output power, under rated terminal voltage conditions, goes to zero. It is desireable to have this speed as high as possible.

The zero output power speed, n_{pu0}, can be determined by substituting $\gamma = 90°$ into (7) and solving for the per unit speed. For a one per unit voltage limit this results in

$$n_{pu0} = \frac{1}{\left| E_0 - X_{ds} I_s \right|} \quad (8)$$

Notice that with one per unit current and motor designs with

$$E_0 = X_{ds} \quad \text{(in per unit)} \quad (9)$$

power output is theoretically obtainable to infinite speed!

It is important to establish what high speed power level is available for motors which satisfy the design rule given in (9). Recall that as the speed increases the stator current must advance in phase (γ increases) in order that the increasing permanent magnet voltage ($n_{pu}E_0$) can be counteracted by demagnetizing armature current ($I_{ds} < 0$). At high speed levels γ approaches $\pi/2$ and can be represented as

$$\gamma = \frac{\pi}{2} - \varepsilon , \quad (10)$$

where ε is a small number. Substituting (10) into (7) results in the

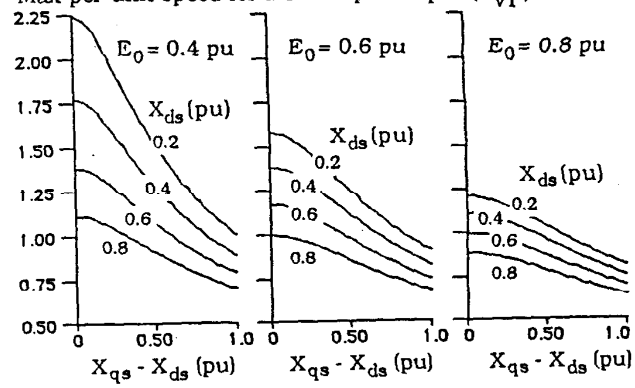

Fig. 9. Speed where one per unit voltage limit is obtained with one per unit current at γ^*.

per unit voltage constraint equation at high speed given below.

$$V_{pu} = n_{pu}\sqrt{(E_0 - X_{ds} I_s \cos\varepsilon)^2 + (X_{qs} I_s \sin\varepsilon)^2} \ . \quad (11)$$

With one per unit voltage and current, ε small and the optimal choice of $E_0 = X_{ds}$, (11) can be used to solve for the operating point ε at a given high speed value giving

$$\varepsilon = \frac{1}{n_{pu} X_{qs}} \ . \quad (12)$$

Substituting (10) into (6) with ε small, $X_{ds} = E_0$ and one per unit current

$$P_{out} = n_{pu} X_{qs} \varepsilon \ . \quad (13)$$

For the high speed ε of (12) the output power with one per unit voltage and current for the optimal design is

$$P_{out} = 1 \text{ per unit.} \quad (14)$$

In other words by chosing $X_{ds} = E_0$ (per unit) with rated current operation the theoretical output power at high speed is the same as the maximum possible output power from the machine. This maximum output power will occur at infinite speed (when ε approaches zero). This says nothing about the power capability at low speed. Obviously the values of X_{qs} and E_0 will have an influence on power capability at low speed. Before going into a detailed analysis of these effects it is useful to consider a motor design which satisfies the design rule of (9).

A. Operating characteristics of optimum designs

Power capability and maximum power output operating characteristics for a motor design which satisfies (9) are plotted in Fig. 10. The current angle asymptotically approaches 90° as the speed increases. Motor power factor and per unit power capability asymptotically approach unity at high speeds. To understand the nature of the power factor variation consider the phasor diagrams for this machine at maximum power output at four speeds as shown in Fig. 11. As the speed increases both V_s and I_s rotate counterclockwise. In the limit, as γ approaches 90°, V_s lies along the negative d axis ($V_{qs} = 0$) since $E_0 - X_{ds}I_s$ would be zero. For all γ slightly less than 90° the motor operates at nearly unity

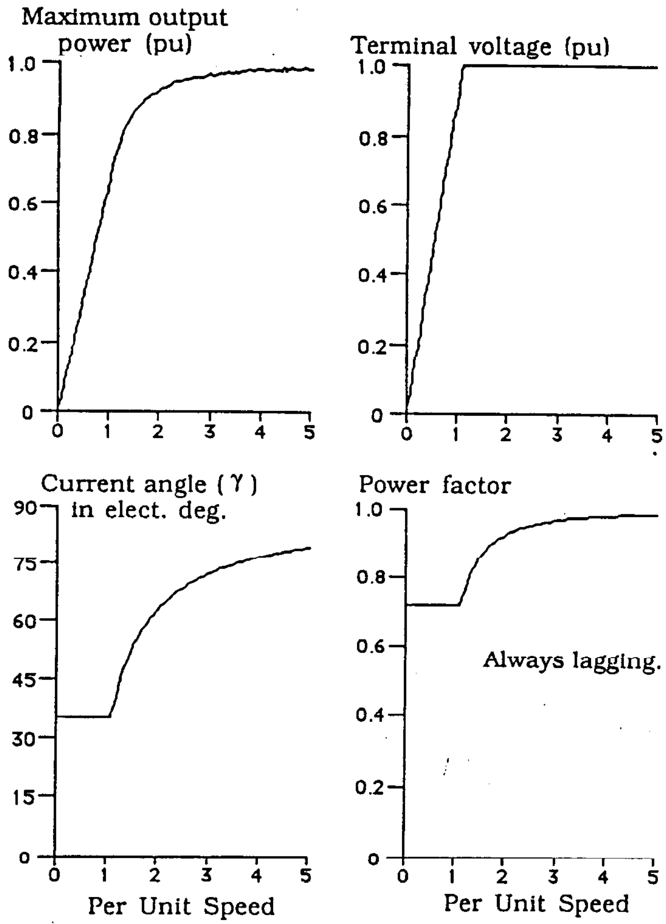

Fig. 10. Operating characteristics at maximum power output for a motor with $X_{ds} = E_0 = 0.4$, $X_{qs} = 1.10$ per unit and 1 per unit current.

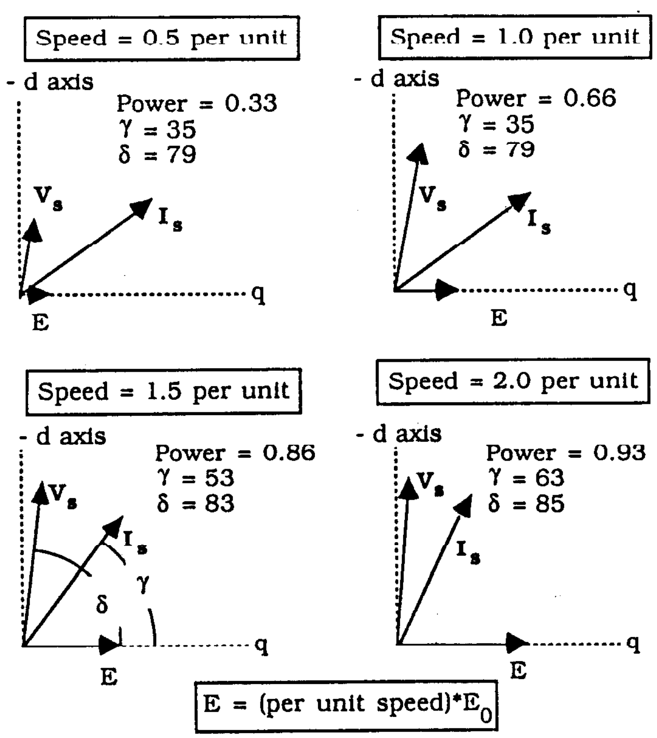

Fig. 11. Phasor diagrams for maximum power output operation for a motor design with $X_{ds} = E_0 = 0.4$, $X_{qs} = 1.1$ per unit.

power factor but always lagging. This is in contrast with the motor design in Fig. 7 where, as the speed increased, V_s rotated clockwise toward the direct axis since E_0 was larger than $X_{ds}I_s$.

The optimal choice of $X_{ds} = E_0$ (per unit) provides high output power capability at high speed yet the level of E_0 as well as the amount of rotor saliency also has an effect on motor power capability at all speeds. In most cases it is desirable to have an adequate level of power capability at rated speed. Fig. 12 shows plots of power capability at rated speed versus rotor saliency and open circuit voltage for motor designs with $X_{ds} = E_0$. The curves were generated assuming rated current (1 per unit) and a one per unit terminal voltage constraint. As expected, the power output at rated speed (or per unit torque) is maximized for designs with the highest possible open circuit voltage and rotor saliency. The incremental increase in power capability with increasing E_0 and saliency decreases as E_0 becomes larger due to the fact that the terminal voltage constraint prohibits operation at the optimal γ ($\gamma = \gamma^*$) for these motor designs.

For speeds above one per unit the voltage constraint becomes more apparent as shown in the power capability curves for 1.5 and 2 per unit speed given in Fig. 13. As the speed increases the power capability gain due to rotor saliency is virtually eliminated for designs with high open circuit voltages.

B. Power capability of near optimal designs

The choice of $X_{ds} = E_0$ (per unit) was shown to optimize motor performance at high speed by theoretically allowing for some output power to infinite speed. For some motor designs with given permanent magnet materials it may not be possible to exactly reach this design objective. It is also important to realize that choosing $X_{ds} = E_0$ only guarantees high output power at high speed. It is conceiveable that other choices of X_{ds} for a given E_0 value may result in better motor performance at lower speeds. Fig. 14 contains rated current power capability curves for five motor designs with the same rotor saliency and E_0 but different values of X_{ds}. Curves 1 and 2 are for machines with $X_{ds} < E_0$ and curves 4 and 5 are for designs with $X_{ds} > E_0$. Curve number 3 is for a machine with the high speed optimal design choice of $X_{ds} = E_0$. It is evident that designs with too low X_{ds} values provide higher low speed power capability than the optimal design (number 3) or those with X_{ds} too large. In fact, design #5 with the largest value of X_{ds} exhibits the lowest power capability at all speeds of all the designs. The high X_{ds} design performance at high speed could be improved by reducing the stator current below one per unit (so that $X_{ds}I_s = E_0$) thereby extending their power capability to high speed. For example, with design #4 and $I_s = 6/7$ pu the asymptotic high speed power capability will be 6/7 per unit. This is less than that obtained with design #3 with one per unit current. In general, motor designs that have too high values of X_{ds} (with respect to (9)) result in lower low speed power capability than those with too low X_{ds} values. This is in agreement with the results presented in Fig. 4.

VI. CONTROL ASPECTS FOR OPERATION BELOW THE POWER CAPABILITY CURVE

Although peak power capability is important it is often necessary to operate at a power level which lies below the power capability curve over a range of speeds. In order to maintain motor operation at peak torque per amp subject to a one per unit voltage constraint it is necessary to simultaneously control the current magnitude and phase as the desired motor output power and speed varies. Fig. 15(a) contains plots of per unit terminal voltage at one per unit speed as a function of current angle and magnitude for a motor design that satisfies (9). Output torque as a function of stator current is given in Fig. 15(b). Notice that the angle for peak torque output for a given current increases with increasing current since

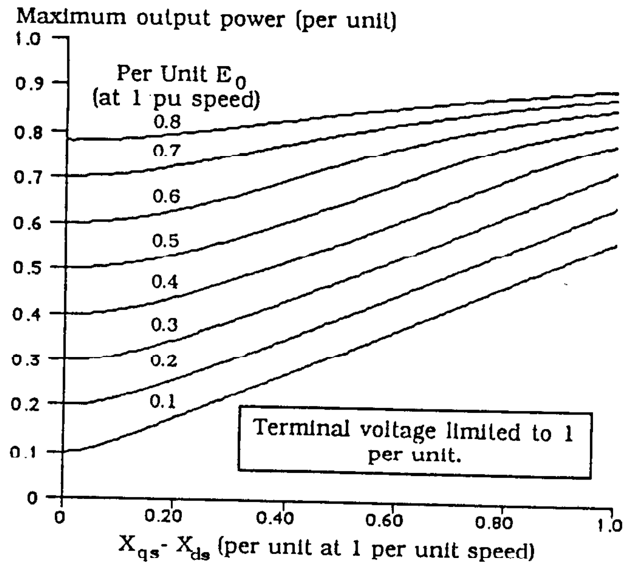

Fig. 12. Power capability at one per unit speed for motor designs with $X_{ds} = E_0$ in per unit with one per unit current.

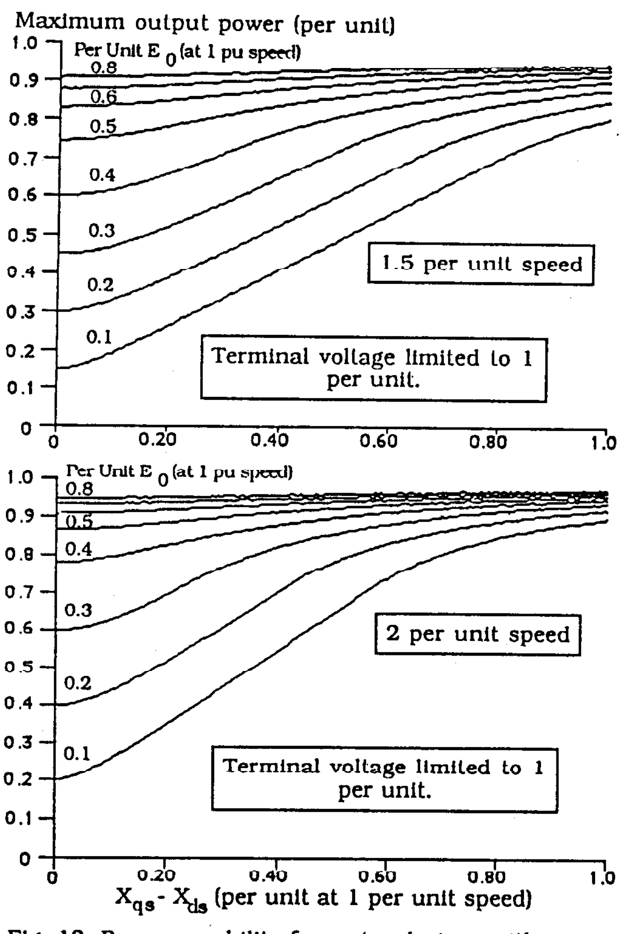

Fig. 13. Power capability for motor designs with $X_{ds} = E_0$ in per unit with one per unit current.

the saliency power (second term of (6)) is proportional to the current squared while the magnet power (first term in (6)) is only proportional to current. At low γ values the voltage increases with the current since most of the armature reaction acts in the quadrature axis to increase the motor flux level. As γ approaches

(per unit at 1 per unit speed)

Design	X_{ds}	X_{qs}	E_0	X_{qs} - X_{ds}
# 1	0.4	0.9	0.6	0.5
# 2	0.5	1.0	0.6	0.5
# 3	0.6	1.1	0.6	0.5
# 4	0.7	1.2	0.6	0.5
# 5	0.8	1.3	0.6	0.5

Terminal voltage limited to 1 per unit at all speeds.

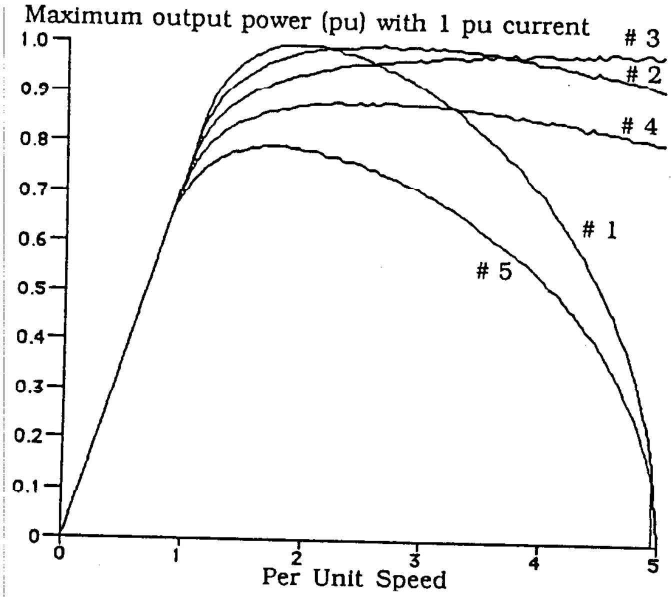

Fig. 14. Power capability curves for five motor designs with 0.5 per unit saliency and 0.6 per unit open circuit voltage and one per unit current.

90° the voltage decreases with increasing current as the armature reaction flux opposes the magnet flux to weaken the motor field.

Terminal voltage is directly proportional to speed for a given current magnitude and angle. At 0.5 per unit speed the motor terminal voltage is less than one per unit at all γ's and current magnitudes. Operation at maximum torque per amp is realized by current control which follows the peaks of the torque versus γ curves as shown in Fig. 15(b). At one per unit speed operation at this optimal current angle is impossible for currents larger than 0.8 per unit without exceeding one per unit voltage. The maximum torque per amp controller must phase advance the current for torque levels above 0.6 per unit.

As the speed increases the maximum torque per amp current angle is dictated by the voltage constraint so that it lies close to 90° for all power levels. Remembering that voltage is proportional to speed, the maximum torque per amp operating points at any speed and current magnitude can be derived from the one per unit speed curves in Fig. 15. These optimal current operating points are plotted for two and three per unit speed in Fig. 15(b). Notice that at three per unit speed and a current magnitude less than 0.4 per unit this motor cannot operate with a terminal voltage less than one per unit at any current angle. The associated output power for peak torque per amp operating points at 1/2, two and three per unit speed can be found by multiplying the output torque obtained from Fig. 15(b) by the corresponding per unit speed. Repeating this process for a variety of output powers results in the current magnitude and angle values for minimum current operation at four motor speeds over a range of power levels as given in Fig. 16. At high speeds very little change in current angle is necessary to obtain a wide change in motor power level.

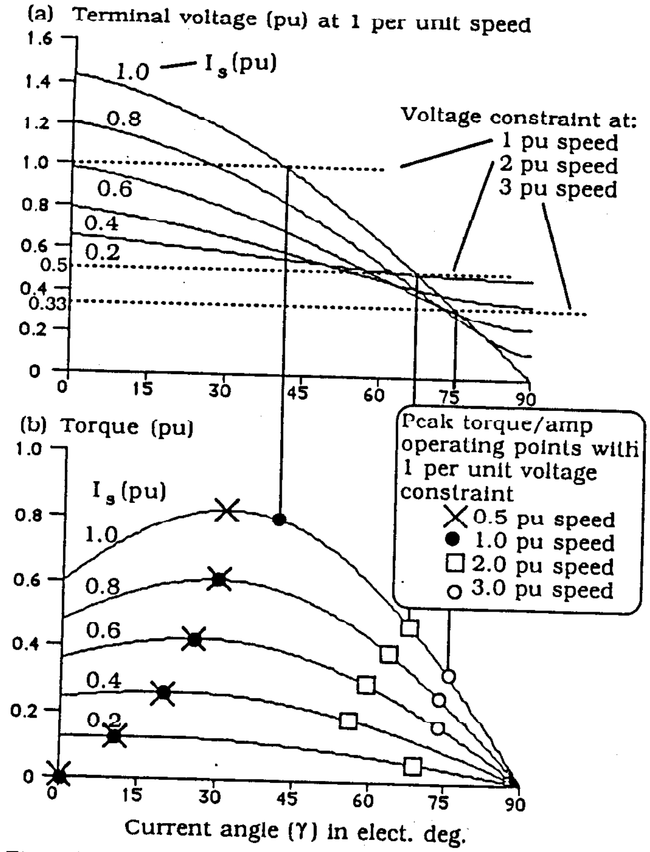

Fig. 15. Operating characteristics of a salient pole motor with X_{qs} = 1.3, X_{ds} = E_0 = 0.6 per unit.

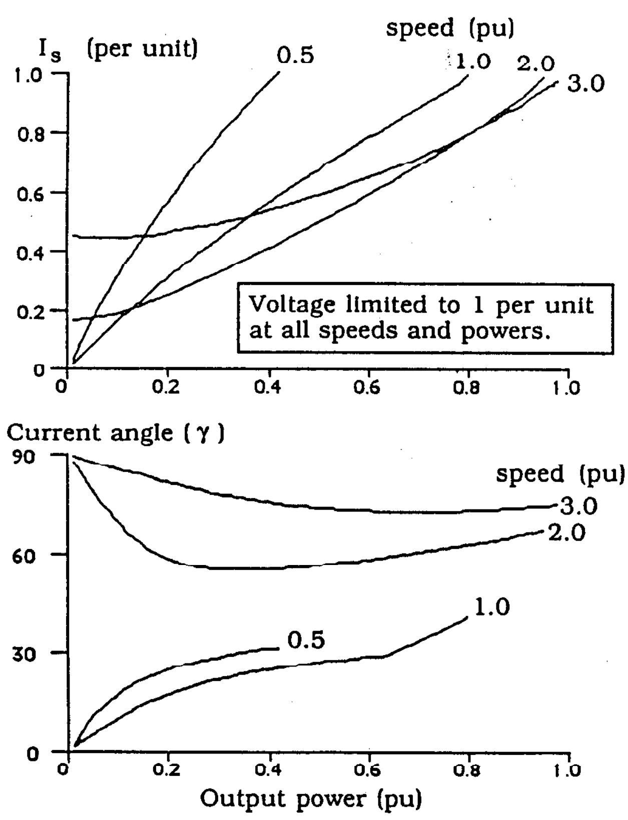

Fig. 16. Current magnitude and angle for peak torque per amp control of motor in Fig. 15.

VII. EFFECTS OF NONIDEAL MOTOR BEHAVIOR

All of the above observations concerning variable speed motor design address the theoretical limits of operation of lossless, salient pole permanent magnet machines without magnetic saturation. Real life motors, naturally, possess some power losses and nonlinearities. The effects of stator IR drop will act to increase the necessary motor voltage above its constant volts per hertz value in order to obtain peak output torque at low speeds. Low speed power capability may also be reduced by the effects of quadrature axis magnetic saturation which acts to reduce X_{qs} at low γ values where the armature reaction lies mostly in the q axis. This will result in a reduction in motor saliency over that predicted with the linear model.

Iron losses become more troublesome as the speed increases since hysteresis loss is roughly proportional to frequency and eddy current loss to frequency squared. At high speed the motor fundamental flux level is quite low so it would be expected that the core loss would not increase at too alarming of a rate. However, in permanent magnet machines, the presence of flux density harmonics created by the magnet and armature reaction fields may add significantly to stator core loss especially at low motor flux levels [11,12,13]. These losses will act to reduce the power capability at high speed and ultimately limit the speed at which power capability drops to zero to something less than the theroretical value of infinity suggested above. If maximum speed operation at constant power is desired, iron losses as well as mechanical losses must be carefully considered in the motor design process.

Iron saturation effects at high speed are not that significant due to the low motor flux level and the fact that armature reaction fields are acting in the direct axis. X_{ds} is relatively independent of the direct axis current for high demagnetizing I_{ds} values [1,9,11] therefore the design rule given in (9) can be maintained over a wide range of high speeds where γ is large.

In buried magnet motors the magnetic nonlinearities are quite extensive, especially in the rotor q axis. Because of this fact it has been suggested that an equivalent circuit model including saturation induced cross coupling reactance is necessary to adequately model the motor. Rotor designs which accentuate this cross coupling effect have been proposed to increase the power capability at high speed in [5]. Unfortunately the effects of this crosscoupling reactance on power capability were demonstrated in [5] through comparisons of designs which had unequal E_0 values. In these comparisons the designs with cross coupling had E_0 values which more closely matched the optimal design rule of (9) than those without crosscoupling. Therefore the increase in power capability can, to some extent, be attributed to the change in E_0 rather than entirely to the cross coupling effect.

VIII. CONCLUSIONS

The power capability of a salient pole, permanent magnet synchronous motor over a wide speed range is a strong function of its equivalent circuit parameters. Peak output torque can be increased with the addition of motor saliency over that obtainable from a nonsalient pole surface magnet motor design. The rated voltage constraint at the motor terminals limits the power output capability at high speed. A tradeoff exists between high peak torque capability at low speed and the speed range over which this peak torque can be maintained before the voltage constraint forces the onset of flux weakening operation. Under flux weakening, for most motor designs, the power capability drops to zero at a particular per unit speed. This upper speed limit can be theoretically extended to infinity if the motor is designed with X_{ds} = E_0 (per unit). With this design choice the maximum possible output power (one per unit) is asymptotically approached as the speed increases. Low speed power capability can be enhanced by increasing the motor open circuit voltage or saliency. If it is not possible to design the motor with $X_{ds} = E_0$ it was shown that it is better, in the power capability sense, to have X_{ds} too low rather than too high.

Peak power capability over a wide speed range is only attainable with independent control of the motor phase current magnitude and angle. This type of control can be used to obtain peak torque per amp operation over a variety of loads and speeds.

IX. REFERENCES

[1] V. Honsinger, "The Fields and Parameters of Interior Type AC Permanent Magnet Machines," IEEE Transactions on Power Apparatus and Systems, Vol. PAS-101, No. 4, April 1982, pp. 867-876.

[2] C. R. Steen, "Direct Axis Aiding Permanent Magnets for a Laminated Synchronous Motor Rotor," United States Patent #4,139,790, February 13, 1979.

[3] T. M. Jahns , G. B. Kliman and T. W. Neumann, "Interior Permanent-Magnet Synchronous Motors for Adjustable-Speed Drives," IEEE Transactions on Industry Applications, Vol. IA-22, No. 4, July/August 1986, pp. 738-747.

[4] T. M. Jahns, "Flux-Weakening Regime Operation of an Interior Permanent-Magnet Synchronous Motor Drive," IEEE Transactions on Industry Applications , Vol. IA-23, No. 4, July/August, 1987, pp. 681-689.

[5] B. Sneyers, D. Novotny and T. A. Lipo, "Field Weakening in Buried Permanent Magnet AC Motor Drives," IEEE Transactions on Industry Applications, Vol. IA-21, No. 2, March/April 1985, pp. 398-407.

[6] B. J. Chalmers, S. A. Hamad and G. D. Baines, "Parameters and Performance of a High-Field Permanent-Magnet Synchronous Motor for Variable Frequency Operation," IEE Proceedings, Vol. 132, B, No. 3, May 1985, pp. 117-124.

[7] T. Sebastian, G. R. Slemon and M. A. Rahman, "Design Considerations for Variable Speed Permanent Magnet Motors," Proceedings of the International Conference on Electrical Machines, Munich, West Germany, September 1986, pp. 1099-1102.

[8] T. Sebastian and G. R. Slemon, "Operating Limits of Inverter-Driven Permanent Magnet Motor Drives," IEEE Transactions on Industry Applications, Vol. IA-23, No. 2, March/April 1987, pp. 327-333.

[9] B. J. Chalmers, S. K. Devgan, D. Howe and W. F. Low, "Synchronous Performance Prediction for High-Field Permanent Magnet Synchronous Motors," Proceedings of the International Conference on Electrical Machines, Munich, West Germany, September 1986, pp. 1067-1070.

[10] E. Richter and T. Neumann, "Saturation Effects in Salient Pole Synchronous Motors with Permanent Magnet Excitation," International Conference on Electrical Machines Conference Record, Lausanne, Switzerland, September 1984, pp. 603-606.

[11] R. Schiferl, "Design Considerations for Salient Pole, Permanent Magnet Synchronous Motors in Variable Speed Drive Applications," Ph. D. Thesis, University of Wisconsin, Madison, Wisconsin, December, 1987.

[12] R. F. Schiferl, R. S. Colby and D. W. Novotny, "Efficiency Considerations in Permanent Magnet Synchronous Motor Drives," Electric Energy Conference (eecon-87) Conference Record, Institute of Engineers, Australia, Adelaide, Australia, October, 1987, pp. 286-291.

[13] R. Schiferl and T. A. Lipo, "Core Loss in Buried Magnet Permanent Magnet Synchronous Motors," IEEE Summer Power Meeting, July, 1988.